A simulation study on the electric field spectral dependence of thunderstorm ground enhancements and gamma ray glows

E. S. Cramer, B. G. Mailyan, Sébastien Celestin, J. R. Dwyer

AGU PUBLICATIONS

JGR

Journal of Geophysical Research: Atmospheres

RESEARCH ARTICLE
10.1002/2016JD026422

Key Points:
- Photon spectra show a variability near the runaway threshold value of the electric field
- We estimate the spectral hardness ratio and intensity dependence on the electric field in thunderclouds
- The variability of the photon spectra means that spectral measurements contain important information on atmospheric electric fields

Correspondence to:
B. G. Mailyan,
bmailyan@fit.edu

Citation:
Cramer, E. S., B. G. Mailyan, S. Celestin, and J. R. Dwyer (2017), A simulation study on the electric field spectral dependence of thunderstorm ground enhancements and gamma ray glows, *J. Geophys. Res. Atmos.*, *122*, 4763–4772, doi:10.1002/2016JD026422.

Received 22 DEC 2016
Accepted 3 APR 2017
Accepted article online 18 APR 2017
Published online 2 MAY 2017

A simulation study on the electric field spectral dependence of thunderstorm ground enhancements and gamma ray glows

E. S. Cramer[1], B. G. Mailyan[1,2,3], S. Celestin[4], and J. R. Dwyer[5]

[1]Center for Space Plasma and Aeronomic Research, University of Alabama in Huntsville, Huntsville, Alabama, USA, [2]Cosmic Ray Division, Yerevan Physics Institute, Yerevan, Armenia, [3]Department of Physics and Space Sciences, Florida Institute of Technology, Melbourne, Florida, USA, [4]LPC2E, University of Orleans, CNRS, Orleans, France, [5]Department of Physics, University of New Hampshire, Durham, New Hampshire, USA

Abstract We have done a thorough simulation analysis on the variability of the photon spectra produced with (due to Relativistic Runaway Electron Avalanche—RREA) and without (Modification of Spectra) the avalanche multiplication process. Despite some measurements obviously showing a variability of the spectra, numerous theoretical studies consider RREA spectrum independent on the electric field. However, analytical calculations by Cramer et al. (2014) have shown that RREA spectrum under low electric fields is not constant and stops being exponential. Using the Relativistic Electron Avalanche Model code, we model various layouts of the electric field configuration and study the predicted photon spectra. The primary focus of the present paper is to study the photon energy spectra, as gamma rays are more often observed by ground-based detectors. The simulation analysis of photon spectra potentially can help to deduce electric fields in thunderclouds.

1. Introduction

The energetic radiation from thunderstorms is currently being measured by ground-based particle detectors worldwide [*Torii et al.*, 2002; *Khaerdinov et al.*, 2005; *Chilingarian et al.*, 2010; *Tsuchiya et al.*, 2011], by means of aircraft [*Kelley et al.*, 2015] and balloon measurements [*Eack et al.*, 2000]. These phenomena can last for tens of minutes and are much longer than submillisecond Terrestrial Gamma-ray Flashes (TGFs) typically observed by spaceborne instruments [*Fishman et al.*, 1994]. The long-lasting fluxes are usually referred as Thunderstorm Ground Enhancements (TGEs) when observed from ground-based detectors or gamma ray glows when observed from airborne detectors.

The understanding of processes leading to the observed particle fluxes was significantly improved during the recent years. A model suggested by *Gurevich et al.* [1992] was proposed to explain the lightning initiation in electric fields lower than conventional breakdown field. The idea was that the atmospheric electric fields accelerate ambient electrons, which produce secondary knock-on electrons and consequently bremsstrahlung photons. *Dwyer* [2003] studied these effects by means of Monte Carlo simulations focusing on the high-energy radiation named Relativistic Runaway Electron Avalanches (RREAs) rather than lightning initiation. The good agreement between the simulations and measurements of TGFs and gamma ray glows suggests that RREA is the probable mechanism of the observed electron and gamma ray production in thunderclouds.

In this study, we will focus on ground-based measurements as they provide an opportunity of constant monitoring of the high-energy atmospheric phenomena in highly active thunderstorm regions, for example, Tampa Bay or Lake Maracaibo in Venezuela [*Albrecht et al.*, 2016]. As electrons rapidly attenuate in the atmosphere, most of the information comes from gamma rays [*Torii et al.*, 2002; *Chilingarian et al.*, 2014; *Tsuchiya et al.*, 2011]. In fact, *Chilingarian et al.* [2014] was the first to suggest that the intracloud electric field during TGEs can be measured based on observing the gamma ray spectrum on the ground. There are only few cases where electrons were measured at the ground level. *Chilingarian et al.* [2012, 2013] were able to estimate the energy spectra of TGE electrons along with gamma ray spectra for the first time. In general, the measurements are in a good agreement with the large-scale RREA model. However, as it was stated in several papers [see, e.g., *Dwyer*, 2004; *Dwyer and Babich*, 2011], the energy spectrum of RREA electrons is expected to have an exponential cutoff at ~7 MeV. Unlike this model prediction, when measuring TGEs, the electron spectra differ from event to event with mean energies that are less than ∼7 MeV. At the same time, the analytical calculations by *Cramer et al.* [2014] showed that RREA energy spectra at low electric fields ($E \approx 286$ kV/m) stop being exponential with ∼7 MeV cutoff and can be described by a convolution of exponential and power law functions. Most interestingly, a dependence of the RREA energy spectra on the atmospheric electric field was found, which explains the measured diversity of the TGEs presented by *Chilingarian et al.* [2012, 2013]. For most of the TGE glows, only gamma ray spectra are possible to estimate. At the same time, the estimations of *Chilingarian et al.* [2014] showed that some of the events correspond to cases where the electric fields are lower than the critical field necessary for the RREA initiation. This process is termed Modification of Spectra (MOS), when secondary cosmic ray electron spectra are modified without an avalanche multiplication process earlier suggested by *Chilingarian et al.* [2012].

In this paper, we will focus on the electric fields below and slightly above RREA threshold to study the variability of the spectra and their dependence on the electric field layout. As there are experimental indications and analytical estimations that RREA electron and gamma ray spectra are varying with the electric field, the RREA particle measurements give a unique possibility to probe atmospheric electric fields. We will discuss the possibilities of the deduction of electric field parameters based on the Monte Carlo simulations by Relativistic Electron Avalanche Model (REAM) [*Dwyer*, 2003, 2004, 2005, 2007, 2008; *Coleman and Dwyer*, 2006]. In addition, we make comparisons with a Monte Carlo code developed by *Celestin and Pasko* [2011].

2. Model Description

In this work, we use the runaway electron avalanche model (REAM) to simulate the production and propagation of high-energy electrons inside thunderstorms. REAM is a Monte Carlo code that includes the relevant cross sections for the interactions of electrons, photons, and positrons with air [*Dwyer*, 2003]. These processes include atomic excitation, Møller scattering, bremsstrahlung emission, pair production, and annihilation. We then study the transport of the resulting X-rays and gamma rays to the observation level. We use an initial population of 10,000 runaway electrons as seeds to the avalanche. The electrons are injected with energies following a secondary cosmic ray power law spectrum. The spectrum is estimated by using the Excel-based Program for calculating Atmospheric Cosmic-ray Spectrum (EXPACS) [*Sato*, 2015]. EXPACS was also used to estimate the seed electron spectrum in *Chilingarian et al.* [2012, 2014]. The power law index of −1.13 was calculated for 5000 m corresponding to typical thundercloud altitudes at Mount Aragats [*Chilingarian et al.*, 2014]. We run several different electric field strengths and acceleration lengths of 500, 1000, and 1500 m. It is worth mentioning that for the sake of future comparisons, these distances were used under sea level density. For instance, because of the similarity of the system under different air densities, at 12 km altitude, 1500 m at sea level corresponds to 6.3 km. This acceleration length is the most extreme case to consider, as we think that larger values are improbable to observe. The electric fields used in the simulation were normalized by the threshold value for which electrons run away, E_{th} = 286 kV/m. This value is higher than the break even field (E_b = 215 kV/m), which is the strength where minimum ionizing electrons lose energy [*Cramer et al.*, 2016]. Note that the calculations to obtain these values are done for an atomic number density of air equal to 5.39×10^{25} atoms/m^3. Values at different altitudes and conditions may be found by scaling these results with the atomic number density. The difference between E_b and E_{th} is due to Coulomb scattering, which increases the path length of the electrons [*Dwyer*, 2004]. Hence, we use the quantity $\delta = E/E_{th}$, where E is the local electric field, to characterize the external field conditions. We specifically study field values slightly above and below E_{th} (i.e., δ is close to 1) in order to compare modeling results with the experimental results of *Chilingarian et al.* [2014] and the theoretical predictions made by *Cramer et al.* [2014].

3. Effects of Electron Propagation Length and Field Strength

Using the model described above, we calculate the resulting photon energy spectrum at the end of the electric field region using different scenarios, dependent on the field length and strength. The hardness ratio of the spectra were calculated to quantify the variability of the photon energy distribution. In Figures 1–3, the spectra (per 10,000 seed electrons) are shown for the electric fields with delta = 1, 1.05, and 1.1, respectively. The blue, black, and red colors are to display the 500 m, 1000 m, and 1500 m field length cases, respectively. For the δ = 1 and length of 500 m case, we obtain a good fit from 2 to 50 MeV by a power law with an index ∼ −1.6, displayed as a green line in Figure 1. With the increase of the field length (potential difference) the spectrum becomes softer as the RREA population grows and starts to dominate the gamma ray emission, but

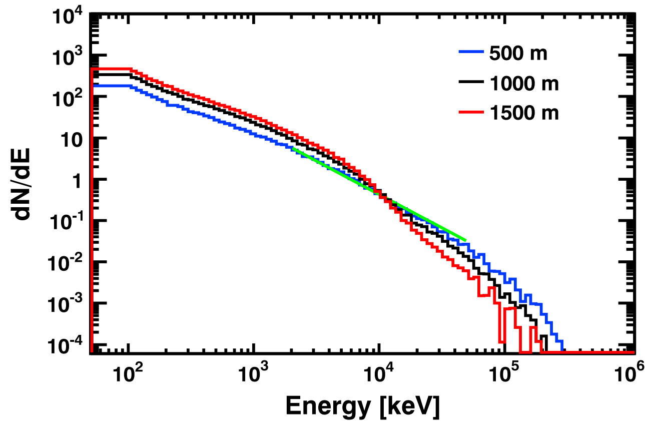

Figure 1. Differential energy spectra of RREA photons for $\delta = 1.0$ case for the field lengths 500 m, 1000 m, and 1500 m. The green line represents the power law fit from 2 to 50 MeV with an index of −1.6.

still can be approximated by a power law function in the configurations studied in the present paper. However, the pattern changes for the higher field strength and lengths. In the case of an electron propagation length of 500 m, the power law index decreases from ≈ -1.6 to ≈ -1.8 for a fit between 2 and 50 MeV when increasing the field from $\delta = 1.0$ to $\delta = 1.05$ (Figure 2). For the $\delta = 1.1$, the gamma ray distribution cannot be well approximated by a power law function and turns to exponential regime as can be seen in Figure 3. For the intermediate potential differences and field strengths the spectra at energies above 1 MeV become a mixture of both power law and exponential distributions. *Cramer et al.* [2014] found that as the electric field approaches the runaway electron threshold value, the solution to the electron energy spectrum is a convolution between a power law function and a Gaussian distribution [see *Cramer et al.*, 2014, equation (39)]. At the same time, it is worth mentioning that even if the power law fits seem not to be correct at relatively high fields above $\delta = 1.05$, as it was shown by *Chilingarian et al.* [2012, 2014], most of the measured TGEs correspond to lower field cases, where power law still applies. Moreover, it was shown that most of the TGEs or glows occur under fields below the runaway threshold, so called Modification of Spectra (MOS) process [*Chilingarian et al.*, 2012]. Without avalanche multiplication, secondary cosmic ray electrons get extra energy from the electric field and due to the increased path lengths emit more gamma rays than without the presence of the electric field in a thundercloud. In Figures 4 and 5, the gamma ray distributions are displayed for the case where the electric field is below the runaway threshold, for $\delta = 0.5$ and $\delta = 0.75$, respectively. Unlike above the RREA threshold cases, when the field length is increased for a certain value of the electric field strength, we have fewer gamma rays reaching the boundary of the region where the electric field is applied in comparison to the shorter field lengths for the same value of the electric field. The attenuation dominates the multiplication in this regime. The situation was opposite for above the RREA threshold cases. At the same time, again, there

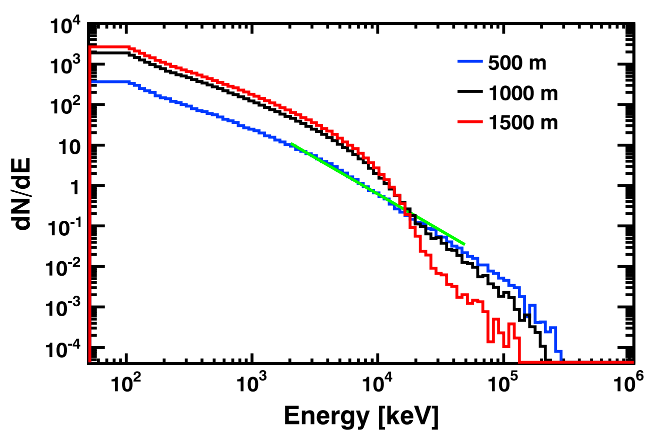

Figure 2. Differential energy spectra of RREA photons for $\delta = 1.05$ case for the field lengths 500 m, 1000 m, and 1500 m. The green line represents the power law fit from 2 to 50 MeV with an index of −1.8.

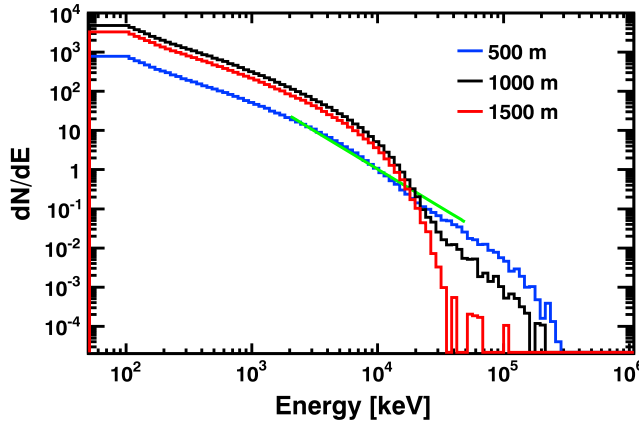

Figure 3. Differential energy spectra of RREA photons for $\delta = 1.1$ case for the field lengths 500 m, 1000 m, and 1500 m. The green line represents the power law fit from 2 to 50 MeV with an index of −1.9.

is a trend of softening of spectra with the increase of the electric field strength. In particular, for an electron propagation length of 500 m, the power law fit between 2 and 50 MeV gives an index of ≈ -1.2 and ≈ -1.3 when increasing the field from $\delta = 0.5$ to $\delta = 0.75$. One can also note that the shape of the spectrum does not change significantly with the electron propagation length for fields $\delta < 1$.

4. Photon Propagation

The next step in our analysis was to propagate the resulting bremsstrahlung photons from the source region to the observation point. Compared to space based observations of TGFs, these ground enhancements experience much less significant atmospheric attenuation. For instance, high-altitude mountainous laboratories such as Aragats allow measurements to be made tens of meters away from the source, which is practically within the thundercloud. Typical thundercloud altitudes from these observation points range from 100 to 200 m. In Figure 6 we present the cases for which $\delta = 0.5$ (below the runaway threshold) and 1.1 (slightly above the runaway threshold). The electric field length for these cases was 1000 m. For the source distances of 100 and 200 m, a decrease of total number of photons can be seen; however, the spectral shape changes are not as significant. Notice that the number of photons below 1 MeV increases between the initial population (RREA) and after the propagation of 100 m through the atmosphere. At this energy range, Compton scattering is the most dominant energy loss process for photons. Due to this scattering process, high-energy photons losing their energy are observed as lower energy particles. However, as the attenuation effect is not as significant than for TGFs, often corrections for propagation are not done assuming the measured spectral shape is the same as the source spectrum [see, e.g., *Tsuchiya et al.*, 2011; *Chilingarian et al.*, 2012].

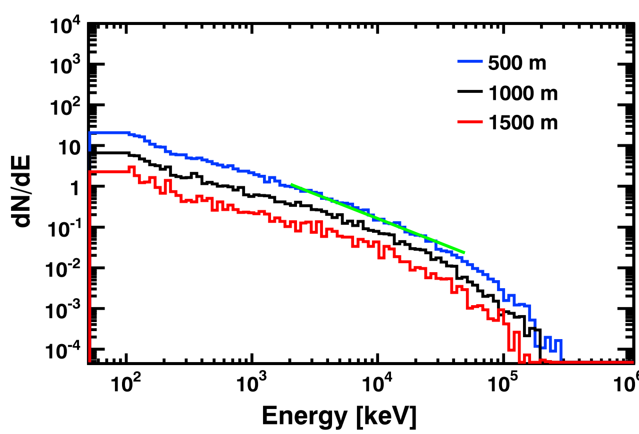

Figure 4. Differential energy spectra of RREA photons for $\delta = 0.5$ case for the field lengths 500 m, 1000 m, and 1500 m. The green line represents the power law fit from 2 to 50 MeV with an index of −1.2.

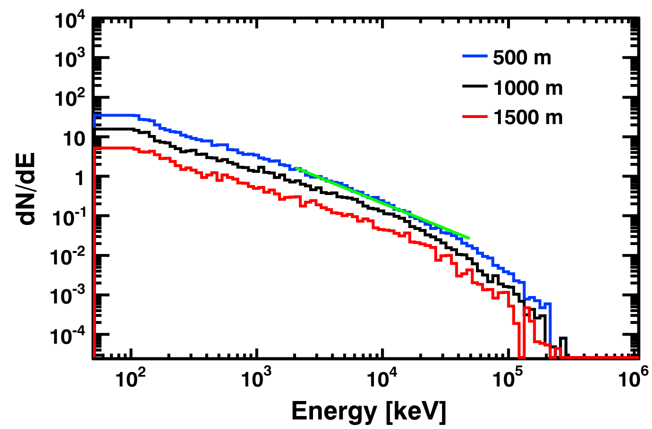

Figure 5. Differential energy spectra of RREA photons for $\delta = 0.75$ case for the field lengths 500 m, 1000 m, and 1500 m. The green line represents the power law fit from 2 to 50 MeV with an index of −1.3.

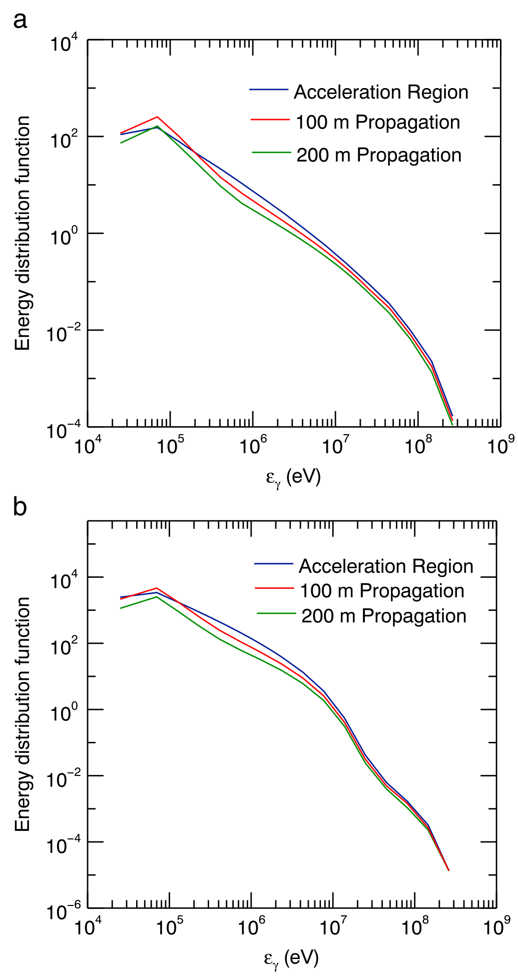

Figure 6. Propagation results of photons from (a) $\delta = 0.5$ and (b) $\delta = 1.1$. The acceleration region was developed over 1000 m and then propagated over 100 and 200 m.

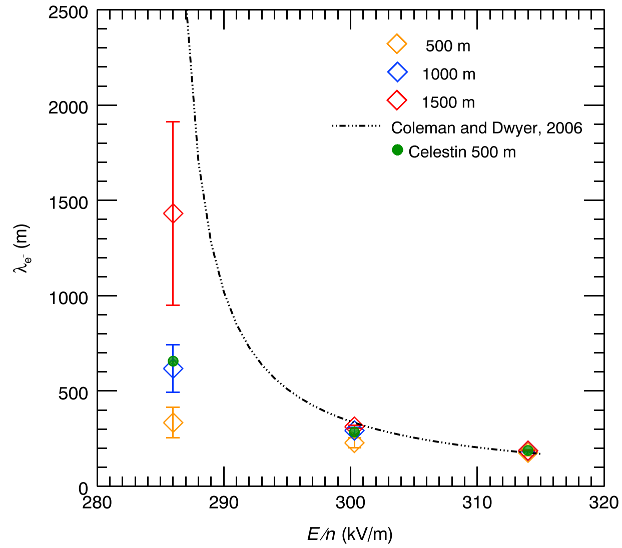

Figure 7. Electron avalanche length as a function of electric field for the three different screen distances of 500 m, 1000 m, and 1500 m. The dashed line is the analytical fit from *Coleman and Dwyer* [2006]. The green circles are estimated by the Monte Carlo code of *Celestin and Pasko* [2011].

It is important to note that for sea level stations, e.g., lightning and thunderstorm active regions such as the Florida or Louisiana coast lines, the corrections for propagation from the source to the observational point are vital as the distances can be as long as several kilometers. These locations are important as they already contain significant scientific infrastructure to study lightning-related phenomena [e.g., *Dwyer et al.*, 2012a; *Ringuette et al.*, 2013].

5. Avalanche Length Calculation

The runaway electron avalanche length is a parameter that represents the average distance an electron travels before the number of runaway electrons is increased by a factor of e (≈2.71) [*Dwyer*, 2003]. This parameter depends on the electric field, as higher strengths will pull more low-energy electrons to the runaway regime, thus decreasing the distance for which more particles are created and/or attenuated. At high electric field values, *Coleman and Dwyer* [2006] showed that the avalanche length can be calculated by the following analytical fit

$$\lambda_{e^-}(E) = \frac{7300\ \text{kV}}{(E - 276)\ \text{kV/m}} \tag{1}$$

However, at lower fields just above the runaway threshold value ($\delta < 1.1$), the following relationship applies

$$\lambda_{e^-}(E) = \frac{5100\ \text{kV}}{(E - 285)\ \text{kV/m}} \tag{2}$$

We compare the current simulation results for $\delta = 1.0$, 1.05, and 1.1 to this analytical equation in Figure 7. As we can see from the figure, there is a large discrepancy between our RREA simulation results and those of *Coleman and Dwyer* [2006] at $\delta = 1.0$, near the threshold field value. Note that equation (2) is not valid for electric fields ≤ 285 kV/m and $\delta = 1.0$ corresponds to a field of 286 kV/m. The different avalanche lengths corresponding to different propagation lengths are obtained in the simulation results and can be explained by the fact that in the field range close to threshold, the avalanche length is on the order of several kilometers. Hence, even for the longest propagation distance used in the present study, the electron distribution does not reach steady state. At the same time, it is important to note that in this work we use a different input energy spectrum from that of *Coleman and Dwyer* [2006] (exponential with an average energy of 7.3 MeV). Therefore, even typical thundercloud field lengths would not be able to produce RREA reaching steady state in this regime. Concurrently, particle fluxes can be observed by ground-based particle detectors even without reaching a steady state, and even below the runaway electron threshold [*Chilingarian et al.*, 2012]. For relatively higher field values, we get agreement with *Coleman and Dwyer* [2006], suggesting the steady state regime has been reached. This is not surprising taking into account the avalanche length for $\delta = 1.05$ and 1.1 is 313 and 186 m, respectively. This means that for the propagation distances we consider here, we are modeling runaway electron propagation through a few avalanche lengths.

6. Discussion and Conclusions

We have done a Monte Carlo simulation study of electron propagation in air under a homogeneous electric field with or without RREA amplification that results in particle enhancements named TGEs or gamma ray glows. Despite the widely discussed ~7 MeV cutoff and independence of the RREA spectrum on the electric field that is usually assumed [see, e.g., *Dwyer*, 2004; *Dwyer and Babich*, 2011], there are some experimental evidences that actually the spectrum is not constant. For example, the measured TGE electron spectra have smaller than predicted ~7 MeV average energy [*Chilingarian et al.*, 2012, 2013]. It should be noted, however, that the 7 MeV cutoff assumption is valid if the RREA reaches a steady state; i.e., the acceleration region is large ($> 5\lambda_{e^-}$). Besides experimental results, there are also analytical calculations indicating the RREA spectrum variability with electric field [*Cramer et al.*, 2014]. *Cramer et al.* [2014] studied the effect of the electric field on the energy spectra of electrons, and the same procedure can be used here to determine the photon spectrum.

At electric fields close to threshold, the bremsstrahlung energy losses are significant and the spectrum becomes a convolution of a power law and exponential function [*Cramer et al.*, 2014]. It was found that the spectrum was sensitive to the value of ε_{max}, which is the uppermost energy an electron can have for a certain electric field value before a balance is reached between the energy gained from the electric field and that lost due to ionization and bremsstrahlung. In *Cramer et al.* [2014], the analysis was done for the runaway electron spectra and the corresponding photon spectrum can be deduced by assuming the bremsstrahlung power law dependence.

In this paper, we have additionally studied the spectral dependence on the electric field length and the effect of the particle passage from source to the detector. A typical distance from the acceleration region to the observational level is on the order of 200 m for most of the observations made at Mount Aragats [*Chilingarian et al.*, 2012]. *Torii et al.* [2004] made Monte Carlo simulations of the particle fluxes from winter thunderstorms in Japan. In Figure 4 of *Torii et al.* [2004], it is shown that the total photon flux near the Lower Positive Charge Region (LPCR) is dominant compared to the field regions above. This is the case of measurements performed at Mount Aragats, and therefore, as a first approximation, only considering the lower charge region is reasonable. As we can see from Figure 6, there are no significant differences in the energy spectra between the acceleration region and the point of observation. Thus, the measured spectrum contains valuable information about the acceleration electric fields.

In Figure 8, we present the dependence of a hardness ratio, defined as the number of photons with energy >10 MeV divided by the number of photons > 1 MeV and < 10 MeV, on the electric field strength. As we mentioned above, the spectrum softens as a result of increased electric field length for $\delta > 0.9$. For the lower values of the electric field strength, the spectrum becomes harder as low-energy photons attenuate in air. We can see from the plot that the hardness ratio is different for various electric field strengths; however, for different potential differences (field lengths), we cannot distinguish the electric fields by measuring only the hardness ratios. For example, the case for which $\delta = 1.05$ and $L = 500$ m gives near the same hardness ratio as the case of $\delta = 1.0$ and $L = 1000$ m. This means to probe the atmospheric electric fields at the time of the gamma ray event, more parameters need to be measured. The degeneracy on field length (total potential difference) should be solved by the observed intensity (see Figure 9), if the distance to the cloud is known. However, in some cases, we can infer the electric field based on the hardness ratio. For example, if a hardness ratio of 0.4 is measured, this should correspond to an electric field close to $0.8E_{th}$.

In Figure 9, the number of photons per 10,000 seed electrons is displayed. As expected, the intensity increases with increasing field strength. Also, it is not surprising that there is an enhancement of the number of particles as the field length increases for $\delta > 0.95$. The effect is opposite and the number of photons decreases for $\delta < 0.95$. This indicates that the true threshold is slightly below the used value for the runaway electron threshold field ($E_{th} = 286$ kV/m), shown in Figure 9 as an intersection of three curves where the number of seed particles equal the number of relativistic electrons at the end of the acceleration region. We possibly can attribute this difference in the simulation to small variations in the multiple scattering cross section, as care should be taken in comparing multiple Monte Carlo codes as discussed in the RREA Simulation Techniques section of *Dwyer et al.* [2012b].

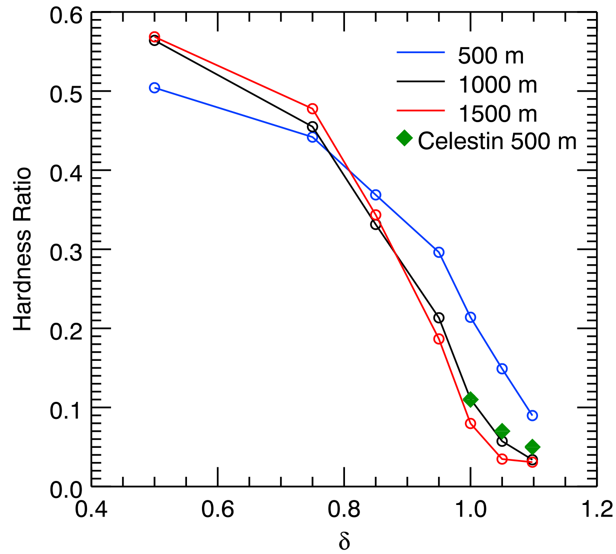

Figure 8. The photon spectral hardness ratio, defined as the number of photons with energy > 10 MeV divided by the number of photons > 1 MeV and < 10 MeV, as a function of electric field (overvoltage). The green diamonds are estimated by the Monte Carlo code of *Celestin and Pasko* [2011].

We present the dependence of the hardness ratio of the photon distribution with photon flux intensity in Figure 10. The hardness ratio for this plot is calculated the same as in Figure 8. The colors of the plot are to indicate the different electric field lengths used in the simulation of 500, 1000, and 1500 m, respectively. The different symbols are to display the various electric field values that were used in the Monte Carlo code. Following the work by *Chilingarian et al.* [2014], we suggest using hardness ratios along with the measured total flux for the recovery of the atmospheric electric fields in thunderclouds. It should be noted that care should be taken when considering lower electric fields ($\delta < 1$) since slight variations of spectra are possible due to the initial electron angular distribution. For higher electric fields ($\delta > 1$), energetic electrons will tend to be aligned with the electric field and the initial cosmic ray angular distribution will not be as essential. As we already mentioned above, the RREA photon spectra are not power law but products of electrons which are distributed by the convolution function of a Gaussian and power law. As we can see from Figure 10, the photon intensity can be a good indicator of the magnitude of the electric field in thundercloud as the hardness ratio alone does not vary much at $\delta = 1.0$ to 1.1. However, for the below threshold electric fields, the hardness

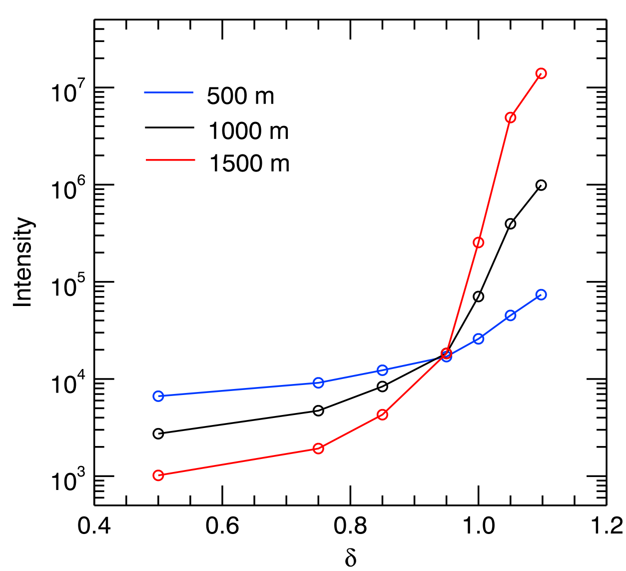

Figure 9. The photon intensity per 10,000 seed electrons as a function of electric field (overvoltage).

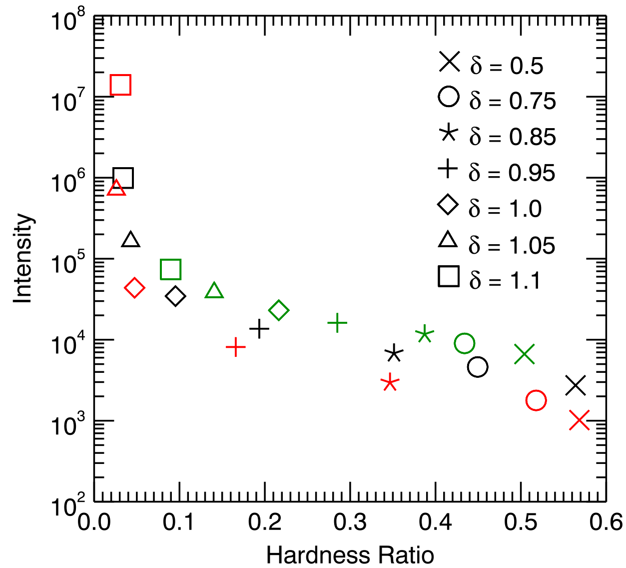

Figure 10. The photon intensity as a function of the hardness ratio. It should be noted that this intensity is produced by 10,000 initial seed electrons. The number of photons above 10 MeV and total number of photons above 1 MeV and less than 10 MeV were used as an estimate for the hardness ratio. The green, black, and red colors represent the field lenghts of 500, 1000, and 1500 m, respectively.

ratio is very sensitive to changes in the field value and has a broader distribution. It is worth mentioning that the intensity spans several orders of magnitudes and the hardness ratio varies between 0.03 and 0.6, which is beneficial for remote sensing the atmospheric electric field. The combination between field length and field strength complicates the estimation of the electric field in the thundercloud, for instance, the case of $\delta = 1.05$ and field length equal to 1500 m can imitate the case of $\delta = 1.1$ and field length of 1000 m. However, within some errors, it is possible to distinguish between cases.

Also, care should be taken as our method should be model independent. Currently, there are many other simulation tools used for high-energy atmospheric physics, e.g., GEANT4 and CORSIKA [*Skeltved et al.*, 2014; *Köhn and Ebert*, 2015]. In Figure 11, we have compared the code from *Celestin and Pasko* [2011] and the REAM Monte Carlo code used in this work. As shown, there is good agreement between the resulting photon energy spectra, which is another step in validating the spectral results obtained by the REAM code.

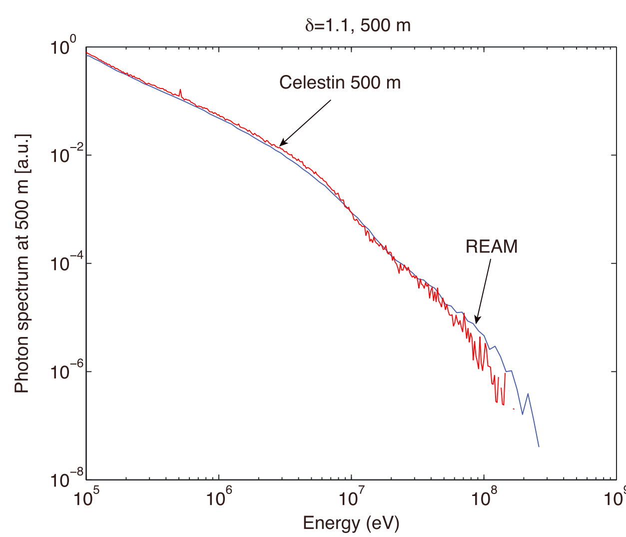

Figure 11. Comparison of Monte Carlo code results from REAM [*Dwyer*, 2007] and *Celestin and Pasko* [2011].

Based on the above estimations, we conclude that particle measurements can give us valuable information about the conditions inside thunderstorm regions. The electric field predictions reported in this work could be tested experimentally if concurrent gamma ray and intracloud measurements were made available. However, for the high-precision quantitative estimates of the electric fields to be deduced from the measured photon spectra, the contributions of other species of secondary cosmic rays should be considered. In addition to lightning detectors that are designed to measure currents and fields on the ground, radiation detectors will significantly improve our understanding of atmospheric physics in lightning active regions.

Acknowledgments
This material is based on work supported by the National Science Foundation under grant 1524533. B.M. thanks NASA Fermi Guest Investigation Program NNX13AO89G. This material is also based in part upon work supported by the Air Force Office of Scientific Research under award FA9550-16-1-0396. Sebastien Celestin is supported by the French space agency (CNES) in the framework of the mission TARANIS. Request for the computer code or data used to generate or be displayed in figures, graphs, or plots may be made to the corresponding author (bmailyan@fit.edu).

References

Albrecht, R. I., S. J. Goodman, D. E. Buechler, R. J. Blakeslee, and H. J. Christian (2016), Where are the lightning hotspots on Earth?, *Bull. Am. Meteorol. Soc.*, *97*, 2051–2068.

Celestin, S., and V. P. Pasko (2011), Energy and fluxes of thermal runaway electrons produced by exponential growth of streamers during the stepping of lightning leaders and in transient luminous events, *J. Geophys. Res.*, *116*, A03315, doi:10.1029/2010JA016260.

Chilingarian, A., A. Daryan, K. Arakelyan, A. Hovhannisyan, B. Mailyan, L. Melkumyan, G. Hovsepyan, S. Chilingaryan, A. Reymers, and L. Vanyan (2010), Ground-based observations of thunderstorm-correlated fluxes of high-energy electrons, gamma rays, and neutrons, *Phys. Rev. D: Part. Fields*, *82*(4), 043009.

Chilingarian, A., B. Mailyan, and L. Vanyan (2012), Recovering of the energy spectra of electrons and gamma rays coming from the thunderclouds, *Atmos. Res.*, *114*, 1–16.

Chilingarian, A., L. Vanyan, and B. Mailyan (2013), Observation of thunderstorm ground enhancements with intense fluxes of high-energy electrons, *Astropart. Phys.*, *48*, 1–7.

Chilingarian, A., G. Hovsepyan, and L. Vanyan (2014), On the origin of the particle fluxes from the thunderclouds: Energy spectra analysis, *Europhys. Lett.*, *106*(5), 59001.

Coleman, L., and J. Dwyer (2006), Propagation speed of runaway electron avalanches, *Geophys. Res. Lett.*, *33*, L11810, doi:10.1029/2006GL025863.

Cramer, E. S., J. R. Dwyer, S. Arabshahi, I. Vodopiyanov, N. Liu, and H. Rassoul (2014), An analytical approach for calculating energy spectra of relativistic runaway electron avalanches in air, *J. Geophys. Res. Space Physics*, *119*, 7794–7823, doi:10.1002/2014JA020265.

Cramer, E. S., J. R. Dwyer, and H. K. Rassoul (2016), Magnetic field modification to the relativistic runaway electron avalanche length, *J. Geophys. Res. Space Physics*, *121*, 11,261–11,270, doi:10.1002/2016JA022891.

Dwyer, J. (2003), A fundamental limit on electric fields in air, *Geophys. Res. Lett*, *30*(20), 2055, doi:10.1029/2003GL017781.

Dwyer, J. (2004), Implications of X-ray emission from lightning, *Geophys. Res. Lett.*, *31*, L12102, doi:10.1029/2004GL019795.

Dwyer, J. (2005), The initiation of lightning by runaway air breakdown, *Geophys. Res. Lett.*, *32*, L20808, doi:10.1029/2005GL023975.

Dwyer, J. (2007), Relativistic breakdown in planetary atmospheres, *Phys. Plasmas*, *14*, 042901.

Dwyer, J. (2008), Source mechanisms of terrestrial gamma-ray flashes, *J. Geophys. Res.*, *113*, D10103, doi:10.1029/2007JD009248.

Dwyer, J., and L. Babich (2011), Low-energy electron production by relativistic runaway electron avalanches in air, *J. Geophys. Res.*, *116*, A09301, doi:10.1029/2011JA016494.

Dwyer, J. R., M. Schaal, E. Cramer, S. Arabshahi, N. Liu, H. Rassoul, J. Hill, D. Jordan, and M. Uman (2012a), Observation of a gamma-ray flash at ground level in association with a cloud-to-ground lightning return stroke, *J. Geophys. Res.*, *117*, A10303, doi:10.1029/2012JA017810.

Dwyer, J. R., D. M. Smith, and S. A. Cummer (2012b), High-energy atmospheric physics: Terrestrial gamma-ray flashes and related phenomena, *Space Sci. Rev.*, *173*(1–4), 133–196.

Eack, K. B., D. M. Suszcynsky, W. H. Beasley, R. Roussel-Dupre, and E. Symbalisty (2000), Gamma-ray emissions observed in a thunderstorm anvil, *Geophys. Res. Lett.*, *27*(2), 185–188.

Fishman, G., P. Bhat, R. Mallozzi, J. Horack, T. Koshut, C. Kouveliotou, G. Pendleton, C. Meegan, R. Wilson, and W. Paciesas (1994), Discovery of intense gamma-ray flashes of atmospheric origin, *Science*, *264*, 1313–1316.

Gurevich, A., G. Milikh, and R. Roussel-Dupre (1992), Runaway electron mechanism of air breakdown and preconditioning during a thunderstorm, *Phys. Lett. A*, *165*(5–6), 463–468.

Kelley, N. A., D. M. Smith, J. R. Dwyer, M. Splitt, S. Lazarus, F. Martinez-McKinney, B. Hazelton, B. Grefenstette, A. Lowell, and H. K. Rassoul (2015), Relativistic electron avalanches as a thunderstorm discharge competing with lightning, *Nat. Commun.*, *6*, 7845.

Khaerdinov, N., A. A. Lidvansky, and V. Petkov (2005), Cosmic rays and the electric field of thunderclouds: Evidence for acceleration of particles (runaway electrons), *Atmos. Res.*, *76*(1), 346–354.

Köhn, C., and U. Ebert (2015), Calculation of beams of positrons, neutrons, and protons associated with terrestrial gamma ray flashes, *J. Geophys. Res. Atmos.*, *120*, 1620–1635, doi:10.1002/2014JD022229.

Ringuette, R., G. L. Case, M. L. Cherry, D. Granger, T. G. Guzik, M. Stewart, and J. P. Wefel (2013), Tetra observation of gamma-rays at ground level associated with nearby thunderstorms, *J. Geophys. Res. Space Physics*, *118*, 7841–7849, doi:10.1002/2013JA019112.

Sato, T. (2015), Analytical model for estimating terrestrial cosmic ray fluxes nearly anytime and anywhere in the world: Extension of parma/expacs, *PLoS One*, *10*(12), e0144679.

Skeltved, A. B., N. Østgaard, B. Carlson, T. Gjesteland, and S. Celestin (2014), Modeling the relativistic runaway electron avalanche and the feedback mechanism with GEANT4, *J. Geophys. Res. Space Physics*, *119*, 9174–9191, doi:10.1002/2014JA020504.

Torii, T., M. Takeishi, and T. Hosono (2002), Observation of gamma-ray dose increase associated with winter thunderstorm and lightning activity, *J. Geophys. Res.*, *107*(D17), 4324, doi:10.1029/2001JD000938.

Torii, T., T. Nishijima, Z.-I. Kawasaki, and T. Sugita (2004), Downward emission of runaway electrons and bremsstrahlung photons in thunderstorm electric fields, *Geophys. Res. Lett.*, *31*, L05113, doi:10.1029/2003GL019067.

Tsuchiya, H., et al. (2011), Long-duration γ ray emissions from 2007 and 2008 winter thunderstorms, *J. Geophys. Res.*, *116*, D09113, doi:10.1029/2010JD015161.